J. Dairy Sci. 104:9931–9947
https://doi.org/10.3168/jds.2021-20187

Effects of varying extracellular amino acid concentrations on bidirectional amino acid transport and intracellular fluxes in mammary epithelial cells

P. S. Yoder,[1,2] J. J. Castro,[3] Tatiana Ruiz-Cortes,[4] and M. D. Hanigan[1]*
[1]Department of Dairy Science, Virginia Polytechnic Institute and State University, Blacksburg 24061
[2]Perdue AgriBusiness LLC, Salisbury, MD 21804
[3]Dairy Visions LLC, Chandler, AZ 85249
[4]Universidad de Antioquia, Faculty of Agricultural Sciences, Research Group Biogenesis, Medellin, Colombia, 050010

ABSTRACT

Understanding the regulation of cellular AA uptake as protein supply changes is critical for predicting milk component yields because intracellular supplies partly regulate protein synthesis. Our objective was to evaluate cellular uptake and kinetic behavior of individual AA when cells are presented with varying extracellular AA supplies. Bovine primary mammary epithelial cells were grown to confluency and transferred to medium with an AA profile and concentration similar to that of plasma from dairy cows for 24 h. Treatments were 4 AA concentrations, 0.36, 2.30, 4.28, and 6.24 m*M*, which represented 16, 100, 186, and 271% of typical plasma AA concentrations, respectively, in lactating dairy cows. Twenty-four plates of cells (89.4 × 19.2 mm) were assigned to each treatment. Cells were first subjected to treatment medium enriched with ^{15}N-labeled AA for 24 h and then incubated with treatment medium enriched with ^{13}C-labeled AA for 0, 15, 60, 300, 900, 1,800, and 3,600 s. Intracellular free AA, intracellular protein-bound AA, and extracellular medium free AA were analyzed for concentrations and isotopic enrichment using gas chromatography–mass spectrometry. A dynamic, 12-pool model was fitted to the data for 14 AA to derive unidirectional uptake and efflux, protein turnover, transamination, oxidation, and synthesis. The derived concentration for half the maximal uptake (k_m) indicated no saturation of AA uptake at typical in vivo concentrations for 11 of the 14 AA. Arginine, Pro, and Val appeared to exhibit saturation kinetics. Net uptake of all essential AA except Phe was positive across treatments. Most nonessential AA exhibited negative net uptake values. Efflux of AA was quite high, with several AA exhibiting greater than 100% efflux of the respective influx. Intracellular pool turnover was rapid for most AA (e.g., 2 min for Arg), demonstrating plasticity in matching needs for protein translation to supplies. Intracellular AA concentrations increased linearly in response to treatment for most AA, whereas 9 AA exhibited quadratic responses. Amino acid uptake is responsive to varying extracellular supplies to maintain homeostasis. No saturation of uptake was evident for most AA, indicating that transporter capacity is likely not a limitation for most AA except possibly Arg, Val, and Pro in mammary epithelial cells.
Key words: amino acid, transport, flux, milk protein

INTRODUCTION

The conversion efficiency of MP to milk protein is not fixed (Doepel et al., 2004), as assumed by common nutrition models (NRC, 2001; Van Amburgh et al., 2015). Varying economic and environmental factors influence the optimum supply of protein required to maximize income over feed costs (Yoder et al., 2016). However, this point cannot be readily determined if nutrition models do not accurately represent the supply–response relationship.

Increasing intracellular concentrations of some EAA stimulates translation rates, resulting in increased milk protein synthesis (Arriola Apelo et al., 2014a,b; Cant et al., 2018). Low intracellular AA concentrations of some AA lead to uncharged transfer RNA, which reduces protein translation and downregulates anabolic signals associated with the general control nonderepressible 2 complex (Ye et al., 2015). Hence, predicting intracellular AA concentrations is important if one wants to predict how milk protein yield responds to changing dietary MP supplies.

Net cellular uptake of AA generally exhibits mass action kinetics within in vivo concentration ranges (Hanigan et al., 1992). Amino acid tracer studies in pig mammary tissue explants indicate linear uptake kinetics within typical in vivo concentration ranges for Val and Lys (Hurley et al., 2000; Jackson et al., 2000). Lin-

Received January 19, 2021.
Accepted March 29, 2021.
*Corresponding author: mhanigan@vt.edu

ear uptake within in vivo concentration ranges was also observed in bovine mammary tissue explants for Arg and Lys (Baumrucker, 1984). These findings suggest that net uptake kinetics might be linear and somewhat inflexible, which implies that reducing dietary MP intake will result in proportional reductions in intracellular AA concentrations and milk protein yield.

Amino acid transporter function has evolved to manage daily AA influx to the translation level precision required for intracellular protein synthesis (Christensen, 1990). System A transporter expression (i.e., SNAT2) was upregulated 25-fold when rat mammary cells were incubated in AA free medium (López et al., 2006), and the regulation appears to be driven by phosphorylation of eukaryotic initiation factor 2 (Gaccioli et al., 2006). Excess AA appeared to downregulate expression of system A transporters in incubated sow mammary tissue (Chen et al., 2018). Sensing of extracellular AA supplies and transmitting of signals via mechanistic target of rapamycin was demonstrated to affect system L transporter SLC7A5 expression (Nicklin et al., 2009; Taylor, 2014). These evaluations of mRNA expression have not evaluated transport rates of individual AA. Most AA kinetic studies also were conducted over such a short time frame (10–30 min) that changes in transport protein activity driven by changes in protein expression would have been insignificant (Pocius and Baumrucker, 1980; Baumrucker, 1984; Hurley et al., 2000; Jackson et al., 2000).

The general promiscuity of AA transporters makes experimental evaluation of functional changes (i.e. conformational changes) of specific transporters to varying substrate concentrations and transport rates difficult to assess. Some transporters are able to transport up to a dozen AA (system L); most AA can be transported by multiple transporter systems; and transport of some AA is driven by sodium gradients, whereas transport of others is driven by the exchange of sodium-dependent transported AA (Christensen, 1990). Incubation of pig mammary tissue with Leu at in vivo concentrations reduced Val uptake by 47% compared with medium without Leu (Jackson et al., 2000). In vivo, additional AA would be competing with Val for system L transporters. The dynamics of multiple transport systems acting in concert to transport AA likely cannot be captured with experiments involving 1 to 2 AA or described by simple linear, univariate uptake equations.

The objective of this study was to assess the kinetics of individual AA uptake using the method described in a companion paper (Yoder et al., 2020a) with multiple AA concentrations varying from below to above the normal in vivo range for lactating dairy cows. Additionally, we aimed to assess efflux and intracellular metabolism of each AA. We hypothesized that unidirectional uptake of AA would exhibit mass action kinetics for all AA within the range of concentrations studied.

MATERIALS AND METHODS

Experimental Design

Bovine primary mammary epithelial cells were obtained from the State Key Laboratory of Animal Nutrition, Institute of Animal Science, Chinese Academy of Agricultural Sciences, Beijing, China. These cells were harvested as previously described (Hu et al., 2009) and verified as previously described (Yoder et al., 2020a). The bovine primary mammary epithelial cells were thawed and plated in fourteen 89.4-mm by 19.2-mm tissue culture-treated polystyrene cell culture dishes (Corning, product no. 353003) at a density of 1.9×10^6 cells/plate. Cells were cultured in growth medium as previously described (Yoder et al., 2020a). Using trypsin (Sigma-Aldrich, no. 59428C), cells were detached from the 2 plates, transferred to a 50-mL canonical tube, and centrifuged at $500 \times g$ for 5 min at 4°C. The resulting supernatant was discarded, and then the pellet was suspended in medium. Cells were then plated in 99 cell culture dishes (89.4 mm × 19.2 mm tissue culture-treated polystyrene) and incubated with the growth medium. Culture dishes were weighed before the addition of cells and medium.

Upon reaching >90% confluency approximately 3 d after plating, cells were incubated for 24 h in a steady-state medium (treatment 2), with AA at concentrations provided in Table 1. These AA concentrations corresponded to what is typically observed in lactating cows (Swanepoel et al., 2016). The medium was changed every 12 h. Following 24-h incubation in the steady-state medium, cells were randomly assigned to one of the 4 treatments (n = 24 plates/treatment). Three plates were retained for background enrichment measurements. Treatments consisted of a constant profile of AA at 4 concentrations of total AA representing 16, 100, 186, and 271% of that observed in lactating cows (Swanepoel et al., 2016; Table 1). The resulting total AA concentrations were 0.36, 2.30, 4.28, and 6.24 m*M* and are abbreviated as **Trt1**, **Trt2** (also the steady-state medium), **Trt3**, and **Trt4**, respectively. All other metabolites were held constant. The target concentrations of AA were achieved using a mix of unlabeled crystalline AA, ^{13}C universally labeled AA derived from algae (U-^{13}C, 97–99% enriched), and ^{15}N universally labeled AA derived from algae (U-^{15}N, 97–99% enriched; Cambridge Isotope Laboratories Inc.) as previously described (Yoder et al., 2020a).

Upon removal of the steady-state medium, cells were washed once with warm PBS and placed in 12 mL of

Table 1. Treatment AA concentrations (μM) in the extracellular medium

	Treatment[1]			
AA	1	2[2]	3	4
Ala	42	268	499	728
Arg	13	80	150	218
Asn	1.2	7.4	14	20
Asp	0.4	2.3	4.2	6.1
Cys	0.4	2.3	4.3	6.3
Glu	8.7	55	102	149
Gln	59	374	695	1,014
Gly	57	358	667	972
His	8.2	52	97	141
Ile	17	108	200	292
Leu	26	165	308	449
Lys	9.0	57	106	154
Met	3.7	24	44	64
Phe	8.2	52	96	140
Pro	16	104	194	283
Ser	15	93	173	251
Thr	17	110	205	298
Trp	12	79	147	214
Tyr	9.2	59	109	159
Val	39	250	466	679
Total	360	2,300	4,280	6,240

[1]Treatment AA profiles mimicked typical lactating dairy cows' plasma (Swanepoel et al., 2016), and total AA concentrations were varied: 16% of in vivo in treatment 1 (0.36 mM), 100% of in vivo in treatment 2 (2.30 mM), 186% of in vivo in treatment 3 (4.28 mM), and 271% of in vivo in treatment 4 (6.24 mM).

[2]Treatment 2 represented the steady-state medium.

^{15}N-enriched treatment medium. Cells were incubated for 24 h with ^{15}N-enriched treatment medium (Supplemental Table S1, http://hdl.handle.net/10919/103853) and fed every 8 h to minimize the effects of the low AA concentration, particularly in Trt1. Following 24 h of incubation, the ^{15}N treatment medium was removed, cells were washed twice with warm PBS, and 6 mL of ^{13}C-enriched treatment medium (Supplemental Table S2, http://hdl.handle.net/10919/103853) was added. Cells and treatment medium were harvested at 0 s, 15 s, 1 min, 5 min, 15 min, 30 min, and 60 min. The zero time point was used to correct for extracellular medium contamination of the cell and plate surfaces (Darmaun et al., 1988). The remaining time points were determined from preliminary experiments. At each harvest time point, the treatment medium was removed and a 1-mL subsample was placed in an ice-cold 1.5-mL tube and stored at −20°C. Cells were rinsed 3 times with ice-cold PBS, the dish plus cells were weighed, and 1 mL of preweighed ice-cold 50% sulfosalicylic acid was added. The plate was gently shaken to ensure rapid cellular lysing, and cell debris was mechanically removed from the plate surface using a cell scraper. The cell lysate was removed to an ice-cold 2-mL tube and stored at −20°C, and the empty culture dish was weighed.

Viable live cells from 3 culture dishes per treatment were counted and weighed to derive weight per cell. Culture dishes were washed twice with warm PBS, the plate was weighed, and 1 mL of 0.05% trypsin EDTA was gravimetrically added to the plate. Upon visible detachment of cells, cells were removed, washed 2 times in PBS, weighed, and resuspended in PBS. Then, a subsample was removed, incubated for 60 min in 0.4% trypan blue (Amresco, no. K940), and counted using a hematocytometer.

The remaining cells from the cell counting plates were centrifuged at 2,500 × g for 5 min. The supernatant was removed, and the cells were lysed in 1 mL of 2% SDS lysis buffer containing phosphatase (Thermo Fisher, no. 78426) and protease (Promega, no. G6521) inhibitors. The resulting homogenate was agitated for 30 min at 4°C and centrifuged for 1 h at 21,130 × g at 4°C to remove insoluble material. The resulting supernatant was assessed for protein content using a bicinchoninic acid assay (Smith et al., 1985) and stored at −80°C.

AA Analyses

The extracellular medium contents were thawed and gravimetrically weighed, acidified with 7% sulfosalicylic acid, and centrifuged at 16,000 × g for 15 min at 4°C. Samples of extracellular medium and intracellular supernatant were gravimetrically combined with ^{13}C^{15}N universally labeled AA (derived from algae, 97–99% enriched; Cambridge Isotope Laboratories Inc.). The cell pellet was gravimetrically combined with ^{13}C^{15}N universally labeled AA and 6 mol of HCl containing 0.1% phenol at 33.3 μL/mg of protein. The sample was blanketed with nitrogen gas, sealed, and acid refluxed at 97.5°C for 20 h to hydrolyze the peptide bonds. Acid hydrolyzed and deproteinized samples were desalted by ion chromatography (AG 50W-X8 resin; Bio-Rad Life Science), eluted with 2 N ammonia hydroxide into silanized glassware, and freeze-dried. Samples were resolubilized in 0.1 N HCl, dried under N for 20 min at 35°C, solubilized in acetonitrile (J. T. Baker Inc.), and converted to N-(tert-butyldimethyl) AA derivatives at 70°C in N-methyl-N-(tert-butyldimethylsilyl)-trifluoroacetamide (Selectra-SIL; UCT Inc.) for 1 h. Amino acid derivatives were separated by GC (Trace GC Ultra; Thermo Scientific), and enrichment of ^{15}N, ^{13}C, and ^{13}C^{15}N ions was determined by MS (DSQII; Thermo Scientific). The sample amounts analyzed by MS for extracellular and intracellular samples were 0.20, 0.09, 0.05, and 0.03 μL for Trt1, Trt2, Trt3, and Trt4, respectively. For all protein-bound samples, the amount was 0.01 μL. This was done to prevent detector

overload resulting in chromatographic peaks that are not Gaussian in shape. Calibration curves for the labeled AA mixture were generated gravimetrically using an AA standard (Sigma-Aldrich, no. AAS18).

Statistical Analysis

A 12-pool, dynamic system of state variables model described in Yoder et al. (2020a) was fit to the resulting data for each AA to derive unidirectional rates of uptake and efflux, catabolism, and incorporation into protein. Initial conditions and starting values were set as described in Yoder et al. (2020a). The "modCost" and "modFit" functions of the FME package (Soetaert and Petzoldt, 2010) were used for fitting to the observed isotope enrichment, AA concentrations, and volume measurements. Residuals were weighted by the overall standard deviation of each variable as previously described (Yoder et al., 2020a). Determination of model structure (i.e., significant parameters) and subsequent evaluation were completed first for Trt2. Model structure did not change for evaluation of other treatments with an AA unless a parameter was no longer significant ($P < 0.10$). Standard errors for parameters and fluxes were determined by Markov chain Monte Carlo with delayed rejection and adaptive Metropolis algorithm (Haario et al., 2006) as described previously (Yoder et al., 2020a). The Markov chain Monte Carlo-generated posterior was sampled 1,000 times (R seed = 123), and the model was solved 1,000 times to generate a population of parameters and fluxes that were used to derive standard errors. Root mean square errors as a percentage of the mean (**RMSE**) and mean square prediction errors partitioned into mean bias, slope bias, and dispersion were calculated for each AA and treatment (Bibby and Toutenberg, 1977). Concordance correlation coefficients (**CCC**) were also calculated to provide a dimensionless evaluation of precision and accuracy.

Hypothesis testing was conducted on concentration- and volume-associated measurements with a model that considered the fixed effect of treatment (4 df), time (6 df), and time by treatment interaction (24 df), and least square derived means were evaluated using linear and quadratic contrast tests. Rate constants and fluxes were statistically evaluated across treatments based on 95% confidence intervals. The mean uptake flux by treatment was standardized to average protein contained in the plate by treatment and AA. This was done by dividing by the mean uptake flux by the mean protein-bound AA mass. The standardized AA uptake fluxes were regressed on extracellular AA concentrations using linear or Michalis-Menten equation forms to derive rate parameters. The latter form was

$$F_{xAAnAA(i)}/Q_{tAA(i)} = \frac{V_m \times C_{xAA(i)}}{k_{(i)} + C_{xAA(i)}},$$

where $F_{xAAnAA(i)}/Q_{tAA(i)}$ represents the unidirectional uptake of the ith AA divided by the ith AA protein-bound pool to standardize the uptake [nmol/min per millimole of protein-bound AA(i)]; $C_{xAA(i)}$ is the extracellular concentration (uM) of the ith AA; V_m is the maximal uptake rate [V_{max}; nmol/s per millimole of protein-bound AA(i)]; and $k_{(i)}$ represents the derived concentration for half the maximal uptake (k_m; uM). Model fit was evaluated for parameter significance, RMSE, CCC, and Bayesian information criterion. If the CCC scores were below 0.50 or RMSE was greater than 40%, the fits were deemed of poor quality and not reliable. Parameters from such models were discarded. The log-likelihood was calculated for each model fit, and likelihood ratio tests were conducted with a chi-squared distribution to derive P-values for model comparisons.

RESULTS

AA Pool Size

Derivation of model parameters required inputs of pool mass, which was determined by multiplication of pool concentration and volume. Extracellular AA concentrations were all linearly affected by treatment ($P < 0.001$; Table 2). A quadratic fit was observed for 12 of the 14 AA ($P = 0.01$); the only 2 AA not exhibiting a quadratic effect were Arg and Asp. Time of exposure to the cells affected the concentration of all AA except Ser ($P < 0.01$). In general, all EAA except Phe exhibited a decline in extracellular AA concentration over the 60-min exposure, whereas all NEAA except Asp increased in medium AA concentrations with Trt4, and some (i.e., Gly and Tyr) increased across all treatments.

Harvested cell weight tended to be affected by treatment ($P = 0.09$), and those effects were linearly related to extracellular AA concentrations ($P = 0.01$; Supplemental Table S3). The increased weight corresponded to differences in cell number ($P = 0.04$), with a linear effect also being observed ($P = 0.01$). Isolated protein weight was affected by treatment ($P < 0.001$) and linearly increased in response to increased extracellular AA supplies ($P < 0.001$). Individual cell weight tended to be affected by treatment ($P = 0.07$) and linearly decreased as extracellular AA supplies increased ($P = 0.03$).

Intracellular free AA concentrations were affected by treatment for all AA except Glu and Gly ($P < 0.01$; Table 3). Thirteen AA increased linearly in concentra-

Table 2. Effect of treatment and time on extracellular free AA concentrations (μM)

	Treatment[2]					*P*-value			
AA[1]	1	2	3	4	SEM	Treatment	Time	Linear[3]	Quadratic[3]
Ala	52[d]	286[c]	498[b]	650[a]	5.6	<0.001	0.002	<0.001	<0.001
Arg	10[d]	66[c]	124[b]	180[a]	2.5	<0.001	<0.001	<0.001	0.98
Asp	4[d]	21[c]	40[b]	51[a]	1.8	<0.001	<0.001	<0.001	0.06
Glu	12[d]	102[c]	163[b]	201[a]	2.2	<0.001	<0.001	<0.001	<0.001
Gly	159[d]	349[c]	497[b]	604[a]	4.6	<0.001	<0.001	<0.001	<0.001
Ile	18[d]	114[c]	198[b]	264[a]	2.2	<0.001	<0.001	<0.001	<0.001
Leu	40[d]	181[c]	313[b]	415[a]	3.4	<0.001	<0.001	<0.001	<0.001
Met	2[d]	19[c]	36[b]	49[a]	0.6	<0.001	<0.001	<0.001	0.01
Phe	18[d]	51[c]	78[b]	92[a]	1.6	<0.001	<0.001	<0.001	<0.001
Pro	21[d]	119[c]	192[b]	246[a]	2.2	<0.001	0.006	<0.001	<0.001
Ser	31[d]	136[c]	220[b]	274[a]	5.0	<0.001	0.85	<0.001	<0.001
Thr	45[d]	161[c]	253[b]	319[a]	2.5	<0.001	0.002	<0.001	<0.001
Tyr	7[d]	38[c]	66[b]	87[a]	0.8	<0.001	0.001	<0.001	<0.001
Val	49[d]	256[c]	445[b]	586[a]	4.6	<0.001	0.002	<0.001	<0.001

[a–d]Least squares means within a row with different superscripts differ ($P < 0.01$).

[1]Concentration includes ^{12}C, ^{13}C, and ^{15}N mass of each AA.

[2]Treatment AA profiles mimicked typical lactating dairy cows' plasma (Swanepoel et al., 2016), and total AA concentrations were varied: 16% of in vivo in treatment 1 (0.36 mM), 100% of in vivo in treatment 2 (2.30 mM), 186% of in vivo in treatment 3 (4.28 mM), and 271% of in vivo in treatment 4 (6.24 mM).

[3]Linear and quadratic contrasts of treatment AA concentrations effects.

tion ($P = 0.05$) as extracellular total AA concentrations increased. Intracellular concentrations of Ala, Asp, Ile, Leu, Phe, Pro, Thr, Tyr, and Val also exhibited quadratic responses ($P < 0.01$), with the apparent plateau occurring between Trt3 and Trt4 for Ala, Asp, Glu, Gly, Ile, Leu, Phe, Pro, Tyr, and Val.

Based on examination of ratios for intracellular to extracellular AA concentrations, the gradient between intracellular and extracellular AA pools varied greatly from a low of 0.5 for Arg to 367 for Glu across treatments. Within Trt2, the average ratio of the concentration gradient was 19.8 for NEAA and 4.2 for EAA, indicating a much higher intracellular concentration of NEAA than EAA relative to extracellular AA pools. The intracellular free AA mass is reported in Supplemental Table S4. All AA linearly increased in mass (*P*

Table 3. Effect of treatment and time on intracellular free AA concentrations (μM)

	Treatment[2]					*P*-value			
AA[1]	1	2	3	4	SEM	Treatment	Time	Linear[3]	Quadratic[3]
Ala	772[b]	3,051[a]	3,350[a]	3,416[a]	221	<0.001	0.84	<0.001	<0.001
Arg	5[c]	46[b]	87[a]	102[a]	19	<0.001	0.51	<0.001	0.45
Asp	231[b]	702[a]	501[b]	547[b]	66	<0.001	<0.001	0.009	0.001
Glu	4,265[b]	5,183[a]	4,670[ab]	4,649[ab]	419	0.55	0.12	0.73	0.25
Gly	3,457[a]	3,200[ab]	2,842[b]	2,751[b]	240	0.11	0.22	0.02	0.72
Ile	69[c]	387[b]	457[a]	464[a]	32	<0.001	0.36	<0.001	<0.001
Leu	147[c]	575[b]	666[a]	674[a]	45	<0.001	0.59	<0.001	<0.001
Met	14[d]	81[c]	141[b]	175[a]	15	<0.001	0.07	<0.001	0.22
Phe	215[b]	362[a]	327[a]	309[a]	28	0.004	0.67	0.05	0.004
Pro	584[b]	2,448[a]	2,372[a]	2,286[a]	181	<0.001	0.09	<0.001	<0.001
Ser	533[c]	896[b]	904[b]	1,158[a]	81	<0.001	0.03	<0.001	0.49
Thr	440[c]	1,104[b]	1,220[ab]	1,319[a]	87	<0.001	0.88	<0.001	0.002
Tyr	141[b]	306[a]	311[a]	313[a]	26	<0.001	0.09	<0.001	0.002
Val	188[b]	967[a]	1,056[a]	981[a]	72	<0.001	0.15	<0.001	<0.001

[a–d]Least squares means within a row with different superscripts differ ($P < 0.01$).

[1]Concentration includes ^{12}C, ^{13}C, and ^{15}N mass of each AA.

[2]Treatment AA profiles mimicked typical lactating dairy cows' plasma (Swanepoel et al., 2016), and total AA concentrations were varied: 16% of in vivo in treatment 1 (0.36 mM), 100% of in vivo in treatment 2 (2.30 mM), 186% of in vivo in treatment 3 (4.28 mM), and 271% of in vivo in treatment 4 (6.24 mM).

[3]Linear and quadratic contrasts of treatment AA concentrations effects.

Table 4. Effect of treatment on intracellular protein-bound AA concentrations (m*M*)

	Treatment[2]					*P*-value
AA[1]	1	2	3	4	SEM	Treatment
Ala	38[a]	27[b]	24[c]	24[c]	0.8	<0.001
Arg	20	20	18	19	1.5	0.48
Asp	92[a]	74[b]	69[c]	67[c]	1.7	<0.001
Glu	153[a]	144[b]	141[b]	135[c]	3.0	0.001
Gly	6[a]	5[b]	4[c]	4[c]	0.2	<0.001
Ile	39	38	38	36	0.9	0.33
Leu	82	80	82	77	3.1	0.70
Met	16	16	15	15	0.7	0.59
Phe	37[a]	37[a]	36[ab]	34[b]	0.7	0.02
Pro	31	29	29	28	1.0	0.24
Ser	11[a]	8[b]	7[b]	7[b]	0.4	<0.001
Thr	21[a]	15[b]	13[c]	13[c]	0.5	<0.001
Tyr	10[a]	6[b]	6[b]	6[b]	0.2	<0.001
Val	44	44	43	42	1.1	0.47

[a–c]Least squares means within a row with different superscripts differ ($P < 0.01$).

[1]Concentration includes ^{12}C, ^{13}C, and ^{15}N mass of each AA.

[2]Treatment AA profiles mimicked typical lactating dairy cows' plasma (Swanepoel et al., 2016), and total AA concentrations were varied: 16% of in vivo in treatment 1 (0.36 m*M*), 100% of in vivo in treatment 2 (2.30 m*M*), 186% of in vivo in treatment 3 (4.28 m*M*), and 271% of in vivo in treatment 4 (6.24 m*M*).

< 0.001), and only Arg, Gly, Met, and Ser did not exhibit quadratic responses to increased extracellular concentrations of AA.

Intracellular protein-bound AA concentrations varied for some AA (i.e., Ala, Asp, Gly, Phe, Ser, Thr, and Tyr; $P < 0.05$) in response to the changing extracellular AA supplies (Table 4). In contrast, Arg, Ile, Leu, Met, Pro, and Val concentrations in protein lysate were unchanged. Intracellular protein-bound AA masses are reported in Supplemental Table S5. All AA were different in mass except Arg and Asp ($P < 0.02$), reflecting the varying volume of the protein lysate pool.

Model Derivation and Fit

Amino acid uptake, efflux, and fast protein turnover rate constants were derived for 14 AA (Table 5; Supplemental Table S6). Transamination, oxidation, slow protein turnover, and fractional synthesis rate constants were derived for some AA. The average coefficient of variation across all treatments, rate constants, and AA was 17.1%. The reported 95% confidence intervals were derived from the posterior distribution generated by Markov chain Monte Carlo simulation (Table 5; Supplemental Table S6). In some cases, the coefficient of variation exceeded 100%, inflecting very low precision of that parameter; however, all parameter estimates were significantly different from 0 ($P < 0.10$; data not shown). The collinearity scores across all treatments and AA were 10 or less, indicating adequate identifiability of parameters with respect to collinearity of the parameters. Consistent with scores of 5 and greater, correlation between some parameters was reasonably high (i.e., >0.90) for influx and efflux coefficients for some AA (data not shown). However, the use of dual isotopes (i.e., ^{13}C and ^{15}N) to simultaneously assess both fluxes enabled parameter identification.

The accuracy and precision of predicted isotope ratios, pool masses, and pool concentrations were assessed. Fit statistics for only the isotope ratio data are shown in Table 6 and Supplemental Table S7. The RMSE in general was greater for Trt1 than for the other treatments. Isoleucine, Val, Ala, Gly, Ser, and Tyr had RMSE less than 25% across all treatments. In general, the RMSE ranged from 10 to 25%. The CCC ranged even more widely, indicating no correlation or explanatory power for some predictions to 0.99 (almost perfect concordance). The low CCC values were particularly evident for predictions of isotope ratios in the slow protein turnover pools, whereas intracellular and extracellular free AA isotope ratios appeared to be explained with good precision and accuracy.

Model Parameters

In general, the rate constants for AA uptake decreased from Trt2 to Trt4 (Table 5; Supplemental Table S6). Treatment differences for AA uptake rate constant were observed for all AA except Ser and Tyr ($P < 0.05$). The efflux rate constant was affected by treatment for all AA except Asp ($P < 0.05$). Treatment influenced the fast turnover rate constant in all EAA but only Glu and Pro among the NEAA ($P < 0.05$). Oxidation rate constants were derived for all AA except

Table 5. Essential AA parameter estimates (min^{-1}) derived by fitting the model to the observed treatment data[1]

	Treatment 1			Treatment 2			Treatment 3			Treatment 4		
Item[2]	Estimate	95% CI	CV	Estimate	95% CI	CV	Estimate	95% CI	CV	Estimate	95% CI	CV
Arg												
UP	0.009^{ab}	0.002–0.015	37.5	0.012^{a}	0.010–0.015	10.8	0.011^{a}	0.010–0.013	7.6	0.006^{b}	0.005–0.007	12.2
EF	0.070^{ab}	0–0.266	142.8	0.095^{ab}	0.031–0.159	34.2	0.118^{a}	0.089–0.146	12.4	0.034^{b}	0–0.070	55.9
OX	0.148^{ab}	0.049–0.246	34.1	0.151^{a}	0.125–0.177	8.7	0.143^{a}	0.121–0.165	7.8	0.100^{b}	0.082–0.119	9.4
TR				0.029	0.013–0.045	27.8	0.023	0.012–0.035	25.8	0.005	0–0.013	87.7
FPT	0.290^{a}	0.248–0.333	7.5	0.038^{b}	0.032–0.043	7.8	0.014^{c}	0.012–0.017	9.2	0.014^{c}	0.012–0.016	6.9
Ile												
UP	0.012^{bc}	0.009–0.015	11.6	0.016^{a}	0.015–0.017	4.2	0.011^{b}	0.010–0.013	6.7	0.007^{c}	0.005–0.009	13.1
EF	0.012^{c}	0.001–0.023	47.8	0.064^{b}	0.063–0.064	0.5	0.073^{a}	0.072–0.073	0.5	0.063^{b}	0.063–0.064	0.4
OX	0.049^{a}	0.040–0.058	9.4	0.036^{ab}	0.030–0.042	8.7	0.030^{b}	0.023–0.036	11.1	0.024^{b}	0.017–0.031	15.1
TR				0.008^{b}	0.007–0.009	8.0	0.010^{a}	0.010–0.011	3.9	0.008^{b}	0.008–0.009	4.1
FPT	0.021^{a}	0.019–0.023	4.8	0.007^{b}	0.004–0.011	21.3	0.007^{b}	0.003–0.010	25.6	0.006^{b}	0.001–0.011	39.8
Leu												
UP	0.012^{bc}	0.008–0.015	13.6	0.018^{ab}	0.016–0.020	6.1	0.015^{b}	0.014–0.016	3.4	0.010^{c}	0.010–0.011	3.7
EF	0.018^{c}	0.002–0.034	45.9	0.087^{b}	0.076–0.097	6.1	0.113^{a}	0.106–0.121	3.3	0.101^{ab}	0.093–0.110	4.2
OX	0.037^{ab}	0.031–0.043	8.6	0.033^{b}	0.029–0.036	4.9	0.027^{bc}	0.024–0.030	5.3	0.022^{c}	0.018–0.026	9.0
TR				0.008	0.007–0.010	8.7	0.010	0.008–0.011	5.8	0.008	0.007–0.009	7.9
FPT	0.024^{ab}	0.021–0.026	5.1	0.019^{b}	0.015–0.023	9.8	0.015^{bc}	0.013–0.017	7.1	0.013^{c}	0.012–0.014	4.7
Met												
UP	0.008^{c}	0.007–0.009	7.1	0.018^{a}	0.016–0.020	6.3	0.014^{ab}	0.012–0.016	5.8	0.011^{b}	0.010–0.012	6.0
EF				0.018^{b}	0.013–0.022	13.4	0.040^{a}	0.033–0.047	9.0	0.041^{a}	0.034–0.048	8.6
OX	0.040^{a}	0.023–0.058	22.0	0.013^{b}	0.009–0.017	13.9	0.003^{c}	0.001–0.006	41.5			
TR	0.012	0–0.024	55.8	0.008	0.005–0.011	18.1	0.003	0.002–0.005	25.5	0.003	0.002–0.005	24.7
FPT	0.034^{a}	0.024–0.043	14.7	0.014^{b}	0.013–0.016	5.9	0.009^{c}	0.008–0.010	5.1	0.007^{c}	0.007–0.008	4.5
Phe												
UP	0.007^{b}	0.002–0.013	40.4	0.028^{a}	0.021–0.034	11.8	0.028^{a}	0.023–0.034	10.2	0.014^{b}	0.011–0.016	8.9
EF	0.025^{b}	0–0.054	59.4	0.121^{a}	0.104–0.138	7.3	0.152^{a}	0.132–0.173	7.0	0.158^{a}	0.136–0.179	6.9
TR	0.001^{b}	0.001–0.002	25.8	0.004^{a}	0.003–0.005	13.6	0.002^{ab}	0.002–0.003	12.4	0.002^{b}	0.001–0.002	15.0
FPT	0.009^{b}	0.009–0.010	3.4	0.010^{b}	0.009–0.011	7.0	0.011^{ab}	0.010–0.012	5.4	0.014^{a}	0.012–0.016	7.2
Thr												
UP	0.004^{c}	0.003–0.005	13.0	0.030^{a}	0.024–0.035	8.9	0.030^{a}	0.025–0.034	7.5	0.020^{b}	0.018–0.022	5.3
EF	0.006^{b}	0.003–0.008	22.9	0.087^{a}	0.070–0.104	10.1	0.119^{a}	0.101–0.137	7.7	0.093^{a}	0.083–0.103	5.4
OX				0.011^{a}	0.008–0.013	10.5	0.005^{b}	0.003–0.006	18.5			
TR	0.001	0.000–0.002	45.8	0.000	0.000–0.001	34.0						
FPT	0.002^{a}	0.002–0.002	10.3	0.001^{b}	0.001–0.001	13.8	0.001^{b}	0.000–0.001	18.5	0.001^{b}	0.001–0.001	15.6
Val												
UP	0.010^{ab}	0.005–0.016	26.7	0.010^{a}	0.010–0.011	4.3	0.006^{b}	0.006–0.007	4.0	0.004^{c}	0.003–0.004	5.3
EF	0.024^{ab}	0–0.054	63.4	0.045^{a}	0.039–0.050	6.1	0.042^{ab}	0.038–0.045	4.8	0.033^{b}	0.029–0.038	6.9
OX	0.033^{a}	0.027–0.039	9.5	0.023^{b}	0.020–0.026	6.4	0.017^{bc}	0.015–0.020	7.3	0.013^{c}	0.010–0.017	12.2
FPT	0.009^{a}	0.007–0.010	7.9	0.004^{b}	0.004–0.005	6.2	0.004^{b}	0.004–0.004	5.8	0.004^{b}	0.003–0.004	5.1

[a–c]Means within a row with different superscripts differ ($P < 0.05$).

[1]Treatment AA profiles mimicked typical lactating dairy cows' plasma (Swanepoel et al., 2016), and total AA concentrations were varied: 16% of in vivo in treatment 1 (0.36 m*M*), 100% of in vivo in treatment 2 (2.30 m*M*), 186% of in vivo in treatment 3 (4.28 m*M*), and 271% of in vivo in treatment 4 (6.24 m*M*). In all treatments, 95% CI was derived from Markov chain Monte Carlo simulation (n = 5,000 runs).

[2]Rate constants: UP = uptake; EF = efflux; OX = oxidation; TR = transamination; FPT = fast protein turnover.

Table 6. Evaluations of predictions of EAA model isotope ratios after the model was fitted by treatment (Trt) to the observed data[1]

		Isotope ratio[3]					
Item	Statistic[2]	E_{nAA}^{13C}	E_{xAA}^{13C}	E_{nAA}^{15N}	E_{xAA}^{15N}	E_{tAA}^{13C}	E_{tAA}^{15N}
Arg							
Trt 1	CCC	0.48	0.48	0.23	0.14	0.80	−0.13
	RMSE	22.2	9.1	26.3	34.5	34.5	4.1
Trt 2	CCC	0.67	0.78	0.85	0.38	0.89	−0.06
	RMSE	16.6	2.7	31.2	26.7	15.7	5.9
Trt 3	CCC	0.25	0.68	0.55	0.86	0.92	0.01
	RMSE	29.0	1.8	92.9	10.3	9.5	6.6
Trt 4	CCC	0.87	0.14	0.22	0.03	0.97	−0.01
	RMSE	23.7	2.5	95.9	96.1	5.9	6.8
Ile							
Trt 1	CCC	0.35	−0.11	0.84	0.23	0.98	0.00
	RMSE	14.8	18.5	6.9	8.2	12.8	4.9
Trt 2	CCC	0.98	0.96	0.96	0.99	0.98	0.03
	RMSE	10.7	3.0	11.1	2.7	13.7	4.9
Trt 3	CCC	0.99	0.97	0.98	0.99	0.98	0.04
	RMSE	8.4	2.0	8.3	2.5	15.5	3.8
Trt 4	CCC	0.98	0.96	0.96	0.99	0.99	0.03
	RMSE	12.2	1.7	12.4	2.6	12.5	3.3
Leu							
Trt 1	CCC	0.16	−0.20	0.92	0.33	0.86	0.00
	RMSE	13.4	15.5	6.9	13.4	39.5	23.3
Trt 2	CCC	0.98	0.97	0.98	0.98	0.94	0.00
	RMSE	9.7	2.9	8.3	4.0	29.1	15.9
Trt 3	CCC	1.00	0.97	0.99	0.99	0.98	0.01
	RMSE	5.3	2.3	5.6	2.7	15.8	12.0
Trt 4	CCC	0.99	0.98	0.96	0.99	0.98	0.02
	RMSE	9.6	1.6	11.9	2.4	14.1	12.6
Met							
Trt 1	CCC	0.47	0.00	0.57	0.00	0.94	−0.08
	RMSE	33.1	19.6	22.6	38.5	9.1	0.9
Trt 2	CCC	0.13	0.77	0.86	0.76	0.99	0.04
	RMSE	29.7	6.2	22.4	12.1	6.7	1.7
Trt 3	CCC	0.95	0.86	0.92	0.82	0.98	0.01
	RMSE	17.2	6.1	10.9	13.2	7.3	2.4
Trt 4	CCC	0.98	0.85	0.84	0.83	0.99	−0.02
	RMSE	13.6	5.7	16.7	13.6	4.7	3.1
Phe							
Trt 1	CCC	0.48	0.86	0.59	0.44	0.99	0.00
	RMSE	44.0	50.0	4.6	7.1	8.4	1.2
Trt 2	CCC	0.95	0.96	0.72	0.89	0.94	0.01
	RMSE	21.2	29.8	13.8	18.3	26.5	1.9
Trt 3	CCC	0.95	0.96	0.90	0.92	0.95	0.00
	RMSE	21.5	24.7	8.2	18.2	25.6	4.2
Trt 4	CCC	0.97	0.96	0.52	0.94	0.97	0.00
	RMSE	18.9	23.7	25.8	15.1	20.1	4.4
Thr							
Trt 1	CCC	0.43	0.37	0.27	0.46	0.88	0.00
	RMSE	17.3	14.1	5.2	8.8	0.9	0.6
Trt 2	CCC	0.82	0.97	0.77	0.80	0.84	0.00
	RMSE	30.4	3.4	2.8	1.2	1.3	1.1
Trt 3	CCC	0.94	0.98	0.97	0.89	0.78	0.00
	RMSE	17.1	2.7	1.6	1.7	1.8	2.0
Trt 4	CCC	0.98	0.99	0.93	0.96	0.79	−0.01
	RMSE	10.4	1.7	2.7	1.0	1.9	2.1
Val							
Trt 1	CCC	0.47	−0.09	0.83	0.52	0.92	0.00
	RMSE	16.0	21.7	8.5	5.5	11.2	6.7
Trt 2	CCC	0.96	0.89	0.96	0.98	0.94	0.03
	RMSE	17.4	2.2	10.8	3.0	10.4	5.5
Trt 3	CCC	0.99	0.88	0.96	0.98	0.97	0.05
	RMSE	6.0	1.5	11.5	2.7	6.4	4.2

Continued

Table 6 (Continued). Evaluations of predictions of EAA model isotope ratios after the model was fitted by treatment (Trt) to the observed data[1]

		Isotope ratio[3]					
Item	Statistic[2]	$E_{nAA}^{^{13}C}$	$E_{xAA}^{^{13}C}$	$E_{nAA}^{^{15}N}$	$E_{xAA}^{^{15}N}$	$E_{tAA}^{^{13}C}$	$E_{tAA}^{^{15}N}$
Trt 4	CCC	0.98	0.70	0.94	0.95	0.97	0.05
	RMSE	9.9	1.8	13.9	3.2	6.5	3.6

[1]Treatment AA profiles mimicked typical lactating dairy cows' plasma (Swanepoel et al., 2016), and total AA concentrations were varied: 16% of in vivo in treatment 1 (0.36 m*M*), 100% of in vivo in treatment 2 (2.30 m*M*), 186% of in vivo in treatment 3 (4.28 m*M*), and 271% of in vivo in treatment 4 (6.24 m*M*).

[2]RMSE = root mean square prediction error; CCC = concordance correlation coefficient.

[3] $E_{nAA}^{^{13}C}$ = $^{13}C/^{12}C$ area ratio of free intracellular AA; $E_{xAA}^{^{13}C}$ = $^{13}C/^{12}C$ area ratio of free media AA; $E_{nAA}^{^{15}N}$ = $^{15}N/^{12}C$ area ratio of free intracellular AA; $E_{xAA}^{^{15}N}$ = $^{15}N/^{12}C$ area ratio of free media AA; $E_{tAA}^{^{13}C}$ = $^{13}C/^{12}C$ area ratio of protein-bound AA; $E_{tAA}^{^{15}N}$ = $^{15}N/^{12}C$ area ratio of protein-bound AA.

Phe and found to be affected by treatment for all AA except Asp ($P < 0.05$). Transamination rate constants were derived for some of the treatments for the EAA and for only Ala and Pro of the NEAA. Treatment differences were only observed for Ile, Phe, and Ala ($P < 0.05$). The AA fractional synthesis rate constant reflecting de novo synthesis was not identifiable with any EAA but was identifiable for all NEAA except Pro. Treatment affected the synthesis rate of Asp, Glu, Gly, and Tyr ($P < 0.05$).

AA Fluxes

Fluxes are reported in Table 7 (EAA) and Supplemental Table S8 (NEAA). The net uptake per minute ranged from −8.4 nmol/min for Gly in Trt1 to +6.4 nmol/min for Ala in Trt2. In general, all EAA exhibited positive net uptake across treatments except for Phe. In contrast, most NEAA had negative net uptake values for several treatments. Net uptake was affected by treatment for all AA except Asp ($P < 0.05$). Unidirectional AA uptake ranged from a low of 0.3 nmol/min for Met in Trt1 to a high of 82.9 nmol/min for Ala in Trt4. Most AA exhibited increases in uptake as extracellular concentrations of AA increased. The AA uptake was affected by treatment for all AA except Glu ($P < 0.05$).

Efflux of AA followed a pattern similar to that of influx, and treatment affected all AA ($P < 0.05$). Fast protein turnover flux was low compared with influx rates and ranged from 0.1 with Met Trt1 to 25.6 nmol/min for Glu Trt3. Treatment affected fast turnover protein flux for all EAA except Thr and only Asp, Glu, and Pro for the NEAA ($P < 0.05$). Transamination fluxes were affected by treatment for only Ile, Leu, Phe, Ala, and Pro ($P < 0.05$). Oxidation fluxes differed by treatment for all AA except Asp and Ser ($P < 0.05$). Last, the fractional AA synthesis flux was affected by treatment for only Asp, Glu, Gly, and Tyr ($P < 0.05$).

AA Uptake Kinetics

The results from regressing AA uptake on extracellular concentrations using linear or Michalis-Menten functions are presented in Table 8 and Figure 1. Arginine, Pro, and Val had k_m values that were less than their respective mean in vivo plasma concentrations. The k_m for Ile was slightly greater than the mean of in vivo concentrations. Of the EAA, Val had by far the lowest $k_{m,}$ at 49% of mean in vivo concentrations. The Michalis-Menten function described the flux data from 11 of the AA as well as or better than the linear function based on RMSE and CCC values. The log-likelihood ratio test indicated that the Michalis-Menten function was more appropriate for all AA except Asp.

AA Pool Turnover

The percent turnover per hour for each pool within treatment and AA is listed in Table 9 and Supplemental Table S9. The extracellular pool completely turned over within the 1-h observation period for Thr, Ala, Gly, Pro, Ser, and Tyr for some treatments. Efflux of Met from the cells was not different than 0 for Trt1, and thus the turnover rate was 0 for that AA and treatment. Compared with the other pools, the intracellular pool had the fastest turnover rate across all AA and treatments in general. For some AA, that pool turned over every 2 min (Arg, Trt1) whereas for other AA, it approached 2.3 h (Glu, Trt1). The fast protein turnover pool was slower, ranging from 3.4%/h for Gly on Trt3 to 423%/h for Glu on Trt3.

Table 7. Essential AA flux predictions[1] (nmol/min) derived from the parameterized model and the treatment (Trt) data[2]

	Net uptake			Uptake			Exit			Turnover			Transamination			Oxidation		
Item	Mean	5% CI	95% CI	Mean	5% CI	95% CI	Mean	5% CI	95% CI	Mean	5% CI	95% CI	Mean	5% CI	95% CI	Mean	5% CI	95% CI
Arg																		
Trt 1	0.4^{c}	0.3	0.4	0.5^{c}	0.2	0.8	0.1^{c}	0.0	0.4	0.6^{ab}	0.5	0.6				0.3^{c}	0.2	0.3
Trt 2	3.0^{b}	2.8	3.2	4.7^{b}	3.8	5.6	1.7^{b}	0.9	2.6	0.7^{a}	0.6	0.7	0.5	0.3	0.7	2.7^{b}	2.5	2.9
Trt 3	4.3^{a}	3.9	4.6	7.6^{a}	6.7	8.6	3.4^{a}	2.7	4.1	0.4^{b}	0.3	0.5	0.7	0.3	1.0	4.1^{a}	3.7	4.5
Trt 4	4.5^{a}	3.9	5.1	5.8^{ab}	4.6	7.1	1.4^{bc}	0.1	2.7	0.6^{ab}	0.5	0.6	0.2	−0.1	0.5	4.1^{a}	3.4	4.7
Ile																		
Trt 1	1.0^{c}	0.9	1.1	1.2^{c}	1.0	1.4	0.2^{c}	0.0	0.4	0.4^{b}	0.3	0.4				0.8^{b}	0.7	0.9
Trt 2	3.6^{a}	3.5	3.8	10.3^{b}	9.6	11.1	6.7^{b}	6.1	7.3	0.8^{a}	0.7	0.8	0.8^{b}	0.7	1.0	3.8^{a}	3.6	4.0
Trt 3	3.6^{a}	3.4	3.9	13.4^{a}	12.5	14.3	9.8^{a}	9.0	10.5	0.9^{a}	0.8	1.0	1.4^{a}	1.2	1.6	4.0^{a}	3.7	4.3
Trt 4	2.8^{b}	2.4	3.3	11.8^{ab}	10.8	12.8	9.0^{a}	8.3	9.7	0.8^{a}	0.8	0.9	1.2^{ab}	0.9	1.4	3.4^{a}	2.9	3.9
Leu																		
Trt 1	1.7^{b}	1.6	1.9	2.4^{c}	1.8	3.0	0.6^{c}	0.1	1.2	0.9^{b}	0.8	0.9				1.3^{b}	1.1	1.5
Trt 2	5.2^{a}	4.9	5.4	18.8^{b}	16.9	20.7	13.6^{b}	11.8	15.4	3.0^{a}	2.5	3.5	1.3^{b}	1.1	1.5	5.1^{a}	4.8	5.4
Trt 3	5.3^{a}	4.9	5.7	28.0^{a}	26.3	29.6	22.6^{a}	21.1	24.2	3.0^{a}	2.6	3.3	1.9^{a}	1.7	2.1	5.4^{a}	5.0	5.8
Trt 4	4.4^{a}	3.8	5.1	26.1^{a}	24.4	27.8	21.7^{a}	20.1	23.3	2.7^{a}	2.5	3.0	1.7^{ab}	1.4	1.9	4.8^{a}	4.1	5.4
Met																		
Trt 1	0.3^{c}	0.2	0.3	0.3^{c}	0.2	0.3				0.1^{b}	0.1	0.2	0.0	0.0	0.1	0.2^{b}	0.1	0.2
Trt 2	0.8^{a}	0.8	0.9	1.4^{b}	1.2	1.5	0.5^{b}	0.4	0.6	0.4^{a}	0.4	0.4	0.2	0.1	0.3	0.4^{a}	0.3	0.4
Trt 3	0.6^{b}	0.5	0.7	2.6^{a}	2.3	2.8	2.0^{a}	1.7	2.3	0.4^{a}	0.4	0.5	0.2	0.1	0.3	0.1^{b}	0.0	0.3
Trt 4	0.4^{bc}	0.3	0.5	2.7^{a}	2.3	3.0	2.3^{a}	1.9	2.6	0.4^{a}	0.4	0.4	0.2	0.1	0.3			
Phe																		
Trt 1	0.0^{a}	−0.1	0.0	1.1^{b}	0.2	2.0	1.2^{b}	0.3	2.1	0.4^{b}	0.4	0.5	0.0^{b}	0.0	0.1			
Trt 2	−0.5^{b}	−0.6	−0.3	8.0^{a}	6.6	9.5	8.5^{a}	7.1	9.9	0.7^{a}	0.7	0.8	0.3^{a}	0.2	0.3			
Trt 3	−0.2^{ab}	−0.4	−0.1	10.5^{a}	8.7	12.2	10.7^{a}	9.0	12.4	0.8^{a}	0.7	0.8	0.2^{ab}	0.1	0.2			
Trt 4	−0.5^{b}	−0.6	−0.4	7.9^{a}	6.6	9.1	8.4^{a}	7.2	9.5	0.7^{a}	0.7	0.8	0.1^{b}	0.1	0.1			
Thr																		
Trt 1	0.4^{c}	0.3	0.5	1.0^{c}	0.8	1.3	0.6^{c}	0.4	0.9	0.2	0.2	0.3	0.1	0.0	0.2			
Trt 2	2.2^{a}	1.9	2.4	27.7^{b}	23.3	32.2	25.6^{b}	21.1	30.0	0.2	0.2	0.3	0.1	0.0	0.2	3.1^{a}	2.7	3.6
Trt 3	1.0^{b}	0.6	1.4	44.9^{a}	38.7	51.1	43.9^{a}	37.8	50.0	0.3	0.2	0.4				1.7^{b}	1.2	2.2
Trt 4	−0.9^{d}	−1.1	−0.6	39.3^{a}	35.5	43.2	40.2^{a}	36.4	44.1	0.3	0.2	0.4					0.0	0.0
Val																		
Trt 1	1.6^{c}	1.4	1.8	2.8^{c}	1.4	4.1	1.1^{b}	−0.2	2.5	0.4^{b}	0.3	0.5				1.6^{c}	1.3	1.8
Trt 2	4.3^{ab}	4.0	4.6	15.6^{a}	14.4	16.8	11.3^{a}	10.3	12.3	1.0^{a}	0.9	1.1				5.8^{a}	5.4	6.2
Trt 3	3.5^{b}	3.0	4.0	16.1^{a}	14.9	17.2	12.5^{a}	11.6	13.5	1.2^{a}	1.1	1.3				5.2^{ab}	4.7	5.8
Trt 4	2.4^{bc}	1.7	3.2	12.8^{b}	11.6	14.0	10.3^{a}	9.3	11.4	1.2^{a}	1.1	1.3				4.1^{b}	3.3	5.0

[a–d]Means within a column with different superscripts differ ($P < 0.05$).

[1]Average flux over 60 min using derived rate constants and experimental data.

[2]Treatment AA profiles mimicked typical lactating dairy cows' plasma (Swanepoel et al., 2016), and total AA concentrations were varied: 16% of in vivo in treatment 1 (0.36 mM), 100% of in vivo in treatment 2 (2.30 mM), 186% of in vivo in treatment 3 (4.28 mM), and 271% of in vivo in treatment 4 (6.24 mM). The 5% and 95% confidence interval SE represents the SD of 1,000 simulated model runs conducted using randomly drawn parameters from Markov chain Monte Carlo-derived parameter posteriors.

Table 8. Evaluation of AA uptake (nmol/mmol of bound protein per minute) given changing extracellular AA concentrations[1]

AA	Model[2]	RMSE	CCC	BIC	*P*-value[3]	Slope	V_{max}	k_m, μM	In vivo,[4] μM
Ala	Linear	11.6	0.98	23.6	—	0.058*	—	—	—
	MM	6.6	0.99	19.2	<0.001		103*	1,130	268
Arg	Linear	34.6	0.77	15.1	—	0.019	—	—	—
	MM	25.9	0.87	12.7	<0.001		5.6	76	80
Asp	Linear	3.7	0.99	−26.6	<0.001	0.001*	—	—	—
	MM	4.7	0.99	−24.7	—		0.3*	49*	2
Glu	Linear	25.9	0.23	−12.3	—	—	—	—	—
	MM	26.8	0.13	−12.1	—	—	—	—	—
Gly	Linear	18.2	0.03	32.9	—	—	—	—	—
	MM	16.3	0.33	32.1	—	—	—	—	—
Ile	Linear	25.2	0.85	13.1	—	0.013*	—	—	—
	MM	14.0	0.95	8.5	<0.001	—	5.9*	114	107
Leu	Linear	20.7	0.91	11.2	—	0.009*	—	—	—
	MM	12.1	0.97	6.9	<0.001	—	6.9*	294	165
Met	Linear	12.6	0.97	1.4	—	0.051*	—	—	—
	MM	10.4	0.98	−0.2	<0.001	—	8.4	122	24
Phe	Linear	38.3	0.54	14.6	—	0.030	—	—	—
	MM	34.3	0.61	13.7	<0.001	—	5.9	74	52
Pro	Linear	37.9	0.52	18.6	—	0.013	—	—	—
	MM	28.5	0.74	16.3	<0.001	—	6.5*	68	104
Ser	Linear	13.8	0.96	27.7	—	0.165*	—	—	—
	MM	8.8	0.98	24.1	<0.001	—	93*	259	93
Thr	Linear	22.0	0.93	29.1	—	0.136*	—	—	—
	MM	21.0	0.93	28.8	<0.001	—	150	891	110
Tyr	Linear	14.7	0.97	15.6	—	0.126*	—	—	—
	MM	9.7	0.99	12.2	<0.001	—	24*	103	59
Val	Linear	32.9	0.97	16.2	—	0.004	—	—	—
	MM	21.3	0.84	12.7	<0.001	—	5.1*	122	250

[1]RMSE = root mean square prediction error percent of mean. CCC = concordance correlation coefficient. BIC = Bayesian information criterion. Slope = slope coefficient for linear model. V_{max} refers to the maximal uptake rate derived from the Michalis-Menten function (units are nmol/mmol of AA protein per minute). k_m refers to the derived AA concentration for half the maximal uptake of AA.

[2]Amino acid uptake was standardized to the protein-bound AA pool of the respective AA and fit to a linear model or Michalis-Menten (MM) function, with the dependent variable being extracellular AA concentration.

[3]*P*-value of log-likelihood ratio test comparison between models. Model with corresponding *P*-value indicates better fit.

[4]Represents typical blood plasma AA concentration in lactating dairy cows (Swanepoel et al., 2016).

*Significant ($P < 0.20$).

DISCUSSION

The primary objective of this experiment was to assess cellular AA entry rates and kinetics given varied extracellular supplies of AA. Intracellular free AA availability partly regulates protein translation (Arriola Apelo et al., 2014b; Cant et al., 2018), and this availability is greatly influenced by AA transport. If AA uptake is completely regulated by demand, then our experimental model is questionable because milk protein demand was likely substantially different in our in vitro model compared with in vivo. Experimental evidence, however, suggests that cellular uptake of AA in short-term experiments occurs independent of intracellular demand. Increasing Ile, Leu, Met, or Thr in mammary tissue slices by 420, 450, 170, and 220 u*M*, respectively, linearly increased these AA concentrations, suggesting that changing concentrations extracellularly translates into increased intracellular AA concentrations (Arriola Apelo et al., 2014a). We expected our treatments to illicit changes in intracellular free AA concentrations partially independent of what intracellular protein synthesis demands over the short-term experiment. However, caution should be exercised as the general expectation is that net uptake would be regulated by intracellular demand, not extracellular supplies.

AA Uptake Kinetics

Saturation or near saturation of uptake within the physiological range is likely for Arg, Pro, and Val, as the observed k_m was less than typical in vivo concentrations. This suggests that transport capacity for these AA may become limiting for milk protein synthesis at greater production levels and that increasing extracellular supplies likely results in diminishing marginal uptake of these AA. Valine is transported by system L transporters, primarily the sodium-independent SLC7A5 and SLC7A8 transporters (Shennan and Boyd, 2014). In a meta-analysis, increasing Val supplies were negatively related to milk protein production (Hanigan et al., 2018). In our study, increasing Val supplies in concert

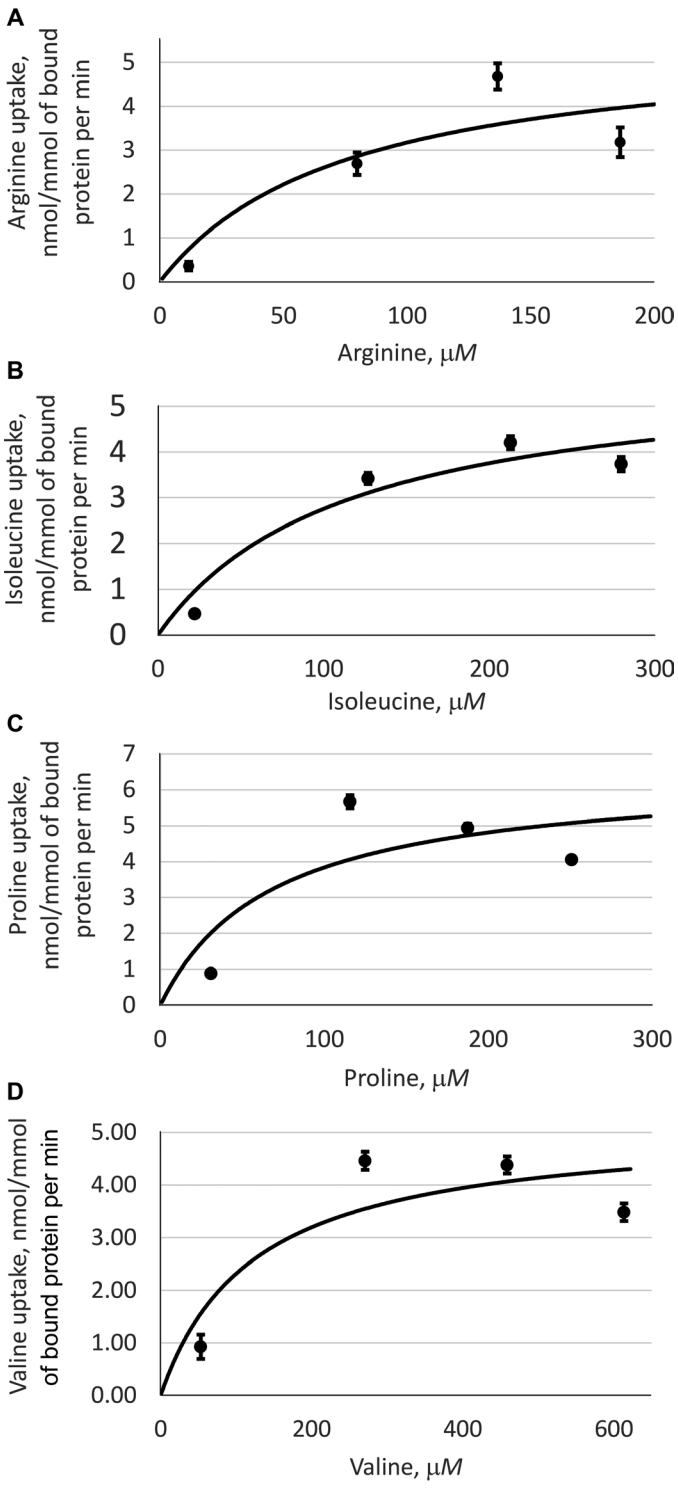

Figure 1. Effect of extracellular AA concentration incubation (24–25 h) on AA unidirectional uptake for arginine (A), isoleucine (B), proline (C), and valine (D). The black circles represent the respective AA uptake standardized to the cellular bound protein mass that was derived from the parameterized model and the treatment data of varying AA concentrations. The SE bars were derived from Markov chain Monte Carlo simulation (n = 1,000). The black solid line represents the Michalis-Menten prediction fitted to the observed parameterized model data.

with total AA supply decreased cellular Val uptake and net uptake and numerically decreased intracellular free Val concentrations. Leucine shares the same transporters as Val, and previously, physiological concentration of Leu (320 u*M*) was shown to inhibit Val uptake by 47% (Jackson et al., 2000). In our experiment, all 20 AA were present and up to 14 AA are known to utilize system L transporters (Wu, 2013; Shennan and Boyd, 2014), so competition likely occurred, thereby potentially limiting Val uptake. The apparent uptake affinity for Val was 10 to 39% lower than the uptake affinity for Leu and Ile despite the fact that that these AA both use the same transporters. The affinity for Leu by system L transporters has been previously observed to be greater than that for Val (Hagenfeldt et al., 1980).

Proline is taken up primarily by sodium-driven system A transporters and is the second most abundant AA in milk protein (Lapierre et al., 2012; Shennan and Boyd, 2014). Alanine, Gly, and Ser are all transported by system A and have been observed to inhibit uptake of Pro by 95 and 87%, respectively (Gay and Hilf, 1980;

Table 9. Turnover (%/h) of media, intracellular free, and intracellular protein-bound EAA pools in response to treatment

	Treatment[1]			
Item	1	2	3	4
Arg				
Extracellular free AA	14.2	27.1	29.8	8.4
Intracellular free AA	3,080	1,774	1,685	937
Fast protein-bound AA	21.4	18.7	10.2	15.7
Ile				
Extracellular free AA	12.2	62.6	50.3	33.8
Intracellular free AA	471	619	627	525
Fast protein-bound AA	27.9	44.1	48.2	43.8
Leu				
Extracellular free AA	18.7	79.2	73.8	51.5
Intracellular free AA	463	810	915	796
Fast protein-bound AA	69.0	179.2	168.2	159.8
Met				
Extracellular free AA		40.5	64.7	55.3
Intracellular free AA	499	360	351	325
Fast protein-bound AA	19.6	46.8	55.6	51.5
Phe				
Extracellular free AA	45.5	176.9	174.4	88.5
Intracellular free AA	171	712	920	921
Fast protein-bound AA	9.3	7.2	5.9	5.1
Thr				
Extracellular free AA	14.3	163.9	173.6	122.4
Intracellular free AA	62.9	568	733	547
Fast protein-bound AA	8.8	9.0	12.1	14.1
Val				
Extracellular free AA	25.7	45.3	28.3	17.2
Intracellular free AA	383	394	343	271
Fast protein-bound AA	29.1	52.2	58.2	56.1

[1]Treatment AA profiles mimicked typical lactating dairy cows' plasma (Swanepoel et al., 2016), and total AA concentrations were varied: 16% of in vivo in treatment 1 (0.36 m*M*), 100% of in vivo in treatment 2 (2.30 m*M*), 186% of in vivo in treatment 3 (4.28 m*M*), and 271% of in vivo in treatment 4 (6.24 m*M*).

Zebisch and Brandsch, 2013). Such transport inhibition by Gly and Ser even occurs during AA starvation (Gay and Hilf, 1980). The increasing concentrations of Gly and Ser might have competitively inhibited Pro uptake, leading to the decline in Pro uptake from Trt2 to Trt4. One of the system A transporters, SNAT2, is adaptively regulated with low concentrations of AA, leading to greater expression (Tovar et al., 2000; Gaccioli et al., 2006; Shennan and Boyd, 2014). In mammary tissue explants, AA free medium increased SNAT2 RNA expression >25-fold versus a complete medium (López et al., 2006). Thus, another possibility is that increased concentrations of AA decreased expression of system A transporters, thereby decreasing Pro uptake. In contrast to Arg and Val, inadequate Pro is taken up by the udder, necessitating synthesis by the mammary gland (Doepel et al., 2016; Yoder et al., 2020b). The needed Pro is synthesized primarily from Arg (Basch et al., 1997), but interestingly, the model parameter for Pro synthesis solved to a value of 0 in the current work. Intracellular Pro concentrations were quite high, with the ratio of intracellular to extracellular concentrations ranging from 9 (Trt4) to 28 (Trt1), which perhaps suppressed synthesis.

The saturation of Arg uptake as total AA concentrations increased suggests that it may be a potential limitation for milk protein synthesis as extracellular AA concentrations increase. Arginine transport is sodium independent and is mediated by 2 different systems: one is specific to cationic AA (system y+) and thought to handle the majority of Arg uptake (80%), and the other handles cationic and neutral AA (system y+L; Sharma and Kansal, 2000; Shennan and Boyd, 2014). Increasing dietary CP supplies in lactating sows decreased expression of CAT-2B, a system y+ transporter, demonstrating adaptive expression (Laspiur et al., 2009). Increasing supplies of Lys also competitively inhibited uptake via system y+ (Baumrucker, 1984). For the other transport system (system y+L), Leu has been shown to be a major competitive inhibitor (Sharma and Kansal, 2000). Because our treatments were applied for a 24-h period before measurement of transport, it is possible that the responses were due to a combination of adaptive regulation (i.e., decreased transporter expression) and competitive inhibition from the increased supplies of AA across treatment.

The calculated k_m of Ile was almost equal to typical in vivo concentrations; hence, transport may approach saturation at the upper range of in vivo concentrations. Increasing supplies of Leu and Ile resulted in curvilinear responses in casein synthesis and phosphorylation of mechanistic target of rapamycin-related proteins in vitro (Arriola Apelo et al., 2014a,b). These declining marginal responses to Leu and Ile supplies may be due to competition for transport resulting in constant or even declining intracellular AA concentrations of other EAA. The lack of positive milk protein responses to branched-chain AA supplementation in dairy cows (Korhonen et al., 2002; Appuhamy et al., 2011; Kassube et al., 2017) may have occurred because of Ile uptake becoming saturated and, as discussed previously, competition by Val for cellular uptake.

Uptake of Ala, Asp, Met, Ser, and Thr appeared to be in the linear range, with derived k_m being 2-fold or more than typical in vivo plasma concentrations. Methionine is transported by a wide range of transport systems that are sodium dependent and independent (Shennan and Boyd, 2014). Perhaps Met being a limiting AA has resulted in the evolution of having various mechanisms for entering the cell and an apparent constant proportional capture of extracellular Met by cells. Threonine is not taken up in excess to milk protein needs, and dietary shortages of Thr elicit substantial changes in blood flow to maintain supplies (Doepel et al., 2016). Like Met, Thr possesses the ability to enter the cell via sodium-dependent or independent transporters, which might explain the lack of apparent saturation of uptake when Thr supplies are increased. Of the 7 EAA we examined in this study, the 2 EAA with the least uptake saturation compared with in vivo concentrations lack transporter specificity and thus have the ability to enter cells using a wide range of transporters.

AA Pools

Mass and concentrations of extracellular AA are subject to net flux across the cell membranes just as are intracellular mass and concentrations. Most extracellular AA concentrations changed less over the course of the incubation period as medium concentrations were increased. This was driven by greater net AA uptake by cells to maintain homeostasis of intracellular free AA when incubated in lower concentrations of AA and a smaller pool of extracellular AA to support cellular use. Cells possess the ability to migrate additional transporters to the cell membrane, change expression of transporters, or posttranslationally modify transport activity to maintain intracellular concentrations (López et al., 2006; Taylor, 2014). The decline in most EAA reflects the inability of cells to synthesize these AA; thus, use and storage result in a net loss to the extracellular pool. Cell storage and demand appear to vary by AA, particularly between EAA and NEAA, which would likely dictate observed intracellular free AA concentrations.

The rapid turnover of the extracellular pool for some AA illustrates the substantial bidirectional transport activity occurring. Previous research with tissue slices

or cells used isotope movement to quantify net uptake (Pocius and Baumrucker, 1980; Baumrucker, 1984; Hurley et al., 2000; Jackson et al., 2000; Shennan et al., 2002). Efflux was not accounted for in these studies. It was apparent in our results that as extracellular concentrations increased with treatment, efflux for many AA was equal to or exceeded uptake of the AA. The prior studies often calculated uptake for kinetic calculations based on intracellular accumulation of the isotope over a short time period (10–30 min). However, even over such a short time period, the high rates of AA efflux from the cells would have resulted in significant intracellular label being returned to the medium, leading to underestimates of transport rates. If our results are extrapolated, linear accumulation of AA intracellularly likely was not occurring as much as inferred in these previous studies because only the isotopically labeled AA was measured, not the ^{12}C form of the AA that was likely being effluxed at a high rate (Pocius and Baumrucker, 1980; Baumrucker, 1984; Hurley et al., 2000; Jackson et al., 2000; Shennan et al., 2002).

The rapid exchange of AA across the cellular membrane resulted in extracellular turnover rates greater than 50%/h for Thr, Ala, Gly, Pro, Ser, and Tyr (Table 9; Supplemental Table S9). Threonine, Ala, and Ser are transported by sodium-independent and dependent mechanisms and likely are important for driving the influx of system L AA, hence the rapid turnover, particularly for Ala and Ser. These results draw into question the implied importance of optimal AA ratios relative to milk protein. Transport clearly changes the profile of AA appearing intracellularly, and this may be done by regulatory control of efflux or at the minimum mass action of efflux. These mechanisms imply a strong capability for transport to take fluctuations in daily intake of AA and profiles and manipulate it to match intracellular needs precisely to what is needed for RNA translation. The reduction in efflux, in some cases to zero (Met) in Trt1, as intracellular AA supplies decline provides a mechanism to increase net uptake independent of extracellular supplies for a particular AA.

Given the complexity of AA transport and the regulation of some transport activity in response to AA supply and profile, it seems unlikely that a single, unique MP profile of AA would be adequate to define milk protein responses. The actions of NEAA on the transport of EAA alone would seem to nullify such efforts. If the EAA profile and ratios of key AA such as Met and Lys all depend on a constant supply and profile of NEAA, then clearly they are not tenable given the complete inattention to predictions of NEAA supplies, synthesis, and concentrations. In support of that conclusion, balancing lactating cow diets to precisely achieve a 3-to-1 ratio of Lys to Met showed no benefit in milk yield across 14 studies in diets with low CP (Sinclair et al., 2014) and does not appear to explain animal responses with high confidence (Hanigan et al., 2000). Identification of the most limiting AA by comparing metabolizable supplies with milk protein yield is inappropriate because transport greatly modifies the intracellular AA profile.

The change in protein-bound AA concentrations due to treatment appears to be isolated to NEAA, with Phe and Thr being the only EAA varying with treatment. Perhaps, because release from lysosomes varies by AA (Abu-Remaileh et al., 2017), the composition of proteins in the fast turnover protein pool is enriched for NEAA, supporting the observation of lack of significance in protein-bound EAA turnover. The difference could also be due to technique. Acid hydrolysis at a single time point results in bias in AA composition. Serine and Thr are more susceptible to destruction in the harsh acid hydrolysis conditions, leading to underestimates of their recovery (Darragh et al., 1996). Our results indicate that this loss during acid hydrolysis clearly occurred for Ser, Gly, and possibly to some extent Thr. To accommodate loss of this pool, the fast protein pool was varied between 1 and 75% for these AA instead of between 1 and 10% to identify optimal model fit. Acid hydrolysis loss of these AA should not have changed the isotope ratio of the pool, only the mass. By using a larger percentage of the protein-bound pool, we achieved good representation of the experimental fast turnover pool size despite a smaller overall pool size caused by acid hydrolysis. Hence, although the protein-bound AA concentrations reported for several AA in Table 4 are most likely incorrect, establishment of a second pool for the fast turnover portion could still be identified.

Parameters, Fluxes, and Turnover

Mass action kinetics of udder AA uptake imply a fixed uptake rate constant regardless of extracellular AA concentrations, which for most AA was not observed because the rate constants were affected by treatment. Increased transporter activity occurs by 2 primary mechanisms: increased affinity for the AA, usually by a conformational change (k_m effect), or increased number of transporter proteins by change in protein expression, protein stability, or movement to the membrane (V_{max} effect; Taylor, 2014; Bröer and Bröer, 2017). Mass action uptake rate constants derived in the 12-pool model were generally the greatest for Trt2 and declined for Tr1, Trt3, and Tr4. These results suggest nonlinear transport with respect to concentra-

tions. This was supported by the generally improved fits for a monomolecular model to the flux and concentration data compared with linear model fits (Table 9). The decrease in affinity for uptake between Trt1 and Tr2 for most AA except Val, Asp, Glu, and Tyr suggests that despite the lowest AA concentrations, no further increases in transporter activity were possible. This might imply maximization of transporter expression or conformational changes. Model fit statistics in almost all parameters and pools were worse for Trt1, so model error in derivation in uptake rate constant may have also occurred. Nevertheless, our results going from Trt4 to Trt2 suggest increased transporter activity. This suggests that as AA concentrations exceed in vivo concentrations, affinity by epithelial cells is diminished, thereby leaving an increased proportion of AA available for splanchnic catabolism. The decreased efficiency in converting absorbed protein into milk protein as increasing amounts of casein are infused has been previously observed (Whitelaw et al., 1986).

Changes in efflux rate constant across treatments were less evident, but increased efflux affinity was generally observed as AA supplies were increased. Efflux regulation is thought to exhibit mass action kinetics (Christensen, 1990). However, efflux is also a function of influx regulation. If more transporters were recruited to the membrane when extracellular supplies were changed, or increased transporter expression occurred, then an increase in apparent rate of efflux should occur. Maximal efflux activity appeared to occur within Trt2 and Trt3 for system L-associated AA, which also corresponded with maximal transporter activity for these AA. In contrast, sodium-independent AA system A did not follow this trend. Some exhibited maximal efflux activity in Trt4 (Ala, Ser), whereas others had small to no changes across Trt (Gly, Pro).

The fast turnover protein synthesis rate constant was highest for Trt1 compared with the other treatments with most of the EAA (Arg, Ile, Leu, Met, and Val). Autophagy is upregulated when cells are depleted of AA and represents a highly conserved mechanisms for maintaining intracellular free AA pools (Mizushima, 2011). The high turnover rate with Trt1 for most EAA likely implies that protein turnover has increased and that degradation of protein might be occurring. In contrast, Pro was the only NEAA to exhibit a significant increase in fast protein turnover in Trt1. Because NEAA can be synthesized by cells, perhaps the need to enhance turnover and degradation of protein to meet NEAA is less evident than for EAA. It is also interesting to consider that when protein supplies are reduced in a dairy cow, increased turnover of EAA may occur to maintain AA supplies for milk protein, which would increase ATP demand in the udder.

CONCLUSIONS

Arginine, Pro, and Val cellular uptakes show saturation or near saturation within the in vivo plasma concentration range of lactating dairy cows. This signifies kinetics akin to a nonlinear function for these AA. Other AA (i.e., Ala, Asp, Met, Ser, and Thr) exhibited uptake kinetics that were clearly mass action, suggesting no saturation within in vivo plasma concentration ranges. Increasing extracellular concentrations largely translated to increased intracellular concentrations, and for most AA, a quadratic effect was observed. This was partially due to declining uptake affinity with increased extracellular concentrations, which indicates that transport efficiency into the cell will decline when protein supplies are increased. Cellular efflux varied greatly (from 0 to 295% of influx). This efflux mechanism helps facilitate intracellular AA supplies to match the precision necessary for RNA translation despite varying extracellular concentrations or imbalanced AA ratios. Transport dynamics suggest that identification of a single, optimal AA profile for dairy cows is possibly a moot objective. In general, the assumption of proportional uptake of AA to varying supplies given that AA are at in vivo concentrations appears to be appropriate for most AA. However, as AA supplies are increased, a declining uptake efficiency will occur for most AA, particularly for Arg, Pro, and Val.

ACKNOWLEDGMENTS

The authors thank Perdue AgriBusiness LLC (Salisbury, MD) via George Betton and Normand St-Pierre for the generous financial support of P. S. Yoder and for funding the experimental work. The authors also appreciate the labor, expertise, and support of Tara Wiles, Evita Huang, and Xinbei Huang (Virginia Tech, Blacksburg, VA). P. S. Yoder designed the experiment and statistical design with the assistance of M. D. Hanigan. The authors have not stated any conflicts of interest.

REFERENCES

Abu-Remaileh, M., G. A. Wyant, C. Kim, N. N. Laqtom, M. Abbasi, S. H. Chan, E. Freinkman, and D. M. Sabatini. 2017. Lysosomal metabolomics reveals V-ATPase- and mTOR-dependent regulation of amino acid efflux from lysosomes. Science 358:807–813. https://doi.org/10.1126/science.aan6298.

Appuhamy, J. A., J. R. Knapp, O. Becvar, J. Escobar, and M. D. Hanigan. 2011. Effects of jugular-infused lysine, methionine, and branched-chain amino acids on milk protein synthesis in high-producing dairy cows. J. Dairy Sci. 94:1952–1960. https://doi.org/10.3168/jds.2010-3442.

Arriola Apelo, S. I., L. M. Singer, X. Y. Lin, M. L. McGilliard, N. R. St-Pierre, and M. D. Hanigan. 2014a. Isoleucine, leucine, methionine, and threonine effects on mammalian target of rapamycin

signaling in mammary tissue. J. Dairy Sci. 97:1047–1056. https://doi.org/10.3168/jds.2013-7348.

Arriola Apelo, S. I., L. M. Singer, W. K. Ray, R. F. Helm, X. Y. Lin, M. L. McGilliard, N. R. St-Pierre, and M. D. Hanigan. 2014b. Casein synthesis is independently and additively related to individual essential amino acid supply. J. Dairy Sci. 97:2998–3005. https://doi.org/10.3168/jds.2013-7422.

Basch, J. J., E. D. Wickham, and H. M. Farrell Jr.. 1997. Arginase in lactating bovine mammary glands: Implications in proline synthesis. J. Dairy Sci. 80:3241–3248. https://doi.org/10.3168/jds.S0022-0302(97)76298-2.

Baumrucker, C. R. 1984. Cationic amino acid transport by bovine mammary tissue. J. Dairy Sci. 67:2500–2506. https://doi.org/10.3168/jds.S0022-0302(84)81606-9.

Bibby, J., and H. Toutenberg. 1977. Prediction and Improved Estimation in Linear Models. Wiley.

Bröer, S., and A. Bröer. 2017. Amino acid homeostasis and signalling in mammalian cells and organisms. Biochem. J. 474:1935–1963. https://doi.org/10.1042/BCJ20160822.

Cant, J. P., J. J. M. Kim, S. R. L. Cieslar, and J. Doelman. 2018. Symposium review: Amino acid uptake by the mammary glands: Where does the control lie? J. Dairy Sci. 101:5655–5666. https://doi.org/10.3168/jds.2017-13844.

Chen, F., S. Zhang, Z. Deng, Q. Zhou, L. Cheng, S. W. Kim, J. Chen, and W. Guan. 2018. Regulation of amino acid transporters in the mammary gland from late pregnancy to peak lactation in the sow. J. Anim. Sci. Biotechnol. 9:35. https://doi.org/10.1186/s40104-018-0250-4.

Christensen, H. N. 1990. Role of amino acid transport and countertransport in nutrition and metabolism. Physiol. Rev. 70:43–77. https://doi.org/10.1152/physrev.1990.70.1.43.

Darmaun, D., D. E. Matthews, J. F. Desjeux, and D. M. Bier. 1988. Glutamine and glutamate nitrogen exchangeable pools in cultured fibroblasts: A stable isotope study. J. Cell. Physiol. 134:143–148. https://doi.org/10.1002/jcp.1041340118.

Darragh, A. J., D. J. Garrick, P. J. Moughan, and W. H. Hendriks. 1996. Correction for amino acid loss during acid hydrolysis of a purified protein. Anal. Biochem. 236:199–207. https://doi.org/10.1006/abio.1996.0157.

Doepel, L., I. I. Hewage, and H. Lapierre. 2016. Milk protein yield and mammary metabolism are affected by phenylalanine deficiency but not by threonine or tryptophan deficiency. J. Dairy Sci. 99:3144–3156. https://doi.org/10.3168/jds.2015-10320.

Doepel, L., D. Pacheco, J. J. Kennelly, M. D. Hanigan, I. F. Lopez, and H. Lapierre. 2004. Milk protein synthesis as a function of amino acid supply. J. Dairy Sci. 87:1279–1297. https://doi.org/10.3168/jds.S0022-0302(04)73278-6.

Gaccioli, F., C. C. Huang, C. Wang, E. Bevilacqua, R. Franchi-Gazzola, G. C. Gazzola, O. Bussolati, M. D. Snider, and M. Hatzoglou. 2006. Amino acid starvation induces the SNAT2 neutral amino acid transporter by a mechanism that involves eukaryotic initiation factor 2α phosphorylation and cap-independent translation. J. Biol. Chem. 281:17929–17940. https://doi.org/10.1074/jbc.M600341200.

Gay, R. J., and R. Hilf. 1980. Influence of proliferative rates and A system substrate availability on proline transport in primary cell cultures of the R3230AC mammary tumor. J. Cell. Physiol. 105:287–300. https://doi.org/10.1002/jcp.1041050212.

Haario, H., M. Laine, A. Mira, and E. Saksman. 2006. DRAM: Efficient adaptive MCMC. Stat. Comput. 16:339–354. https://doi.org/10.1007/s11222-006-9438-0.

Hagenfeldt, L., S. Eriksson, and J. Wahren. 1980. Influence of leucine on arterial concentrations and regional exchange of amino acids in healthy subjects. Clin. Sci. (Lond.) 59:173–181. https://doi.org/10.1042/cs0590173.

Hanigan, M. D., C. C. Calvert, E. J. DePeters, B. L. Reis, and R. L. Baldwin. 1992. Kinetics of amino acid extraction by lactating mammary glands in control and sometribove-treated Holstein cows. J. Dairy Sci. 75:161–173. https://doi.org/10.3168/jds.S0022-0302(92)77750-9.

Hanigan, M. D., J. France, L. A. Crompton, and B. J. Bequette. 2000. Evaluation of a representation of the limiting amino acid theory for milk protein synthesis. Pages 127–144 in Modelling Nutrient Utilization in Farm Animals. J. P. McNamara, J. France, and D. Beever, ed. CABI.

Hanigan, M. D., H. Lapierre, R. Martineau, and A. M. Myers. 2018. Predicting milk protein production from amino acid supply. J. Dairy Sci. 101(E-Suppl. 2):410. (Abstr.)

Hu, H., J. Wang, D. Bu, H. Wei, L. Zhou, F. Li, and J. J. Loor. 2009. In vitro culture and characterization of a mammary epithelial cell line from Chinese Holstein dairy cow. PLoS One 4:e7636. https://doi.org/10.1371/journal.pone.0007636.

Hurley, W. L., H. Wang, J. M. Bryson, and D. B. Shennan. 2000. Lysine uptake by mammary gland tissue from lactating sows. J. Anim. Sci. 78:391–395. https://doi.org/10.2527/2000.782391x.

Jackson, S. C., J. M. Bryson, H. Wang, and W. L. Hurley. 2000. Cellular uptake of valine by lactating porcine mammary tissue. J. Anim. Sci. 78:2927–2932. https://doi.org/10.2527/2000.78112927x.

Kassube, K. R., J. D. Kaufman, K. G. Pohler, J. W. McFadden, and A. G. Rius. 2017. Jugular-infused methionine, lysine and branched-chain amino acids does not improve milk production in Holstein cows experiencing heat stress. Animal 11:2220–2228. https://doi.org/10.1017/S1751731117001057.

Korhonen, M., A. Vanhatalo, and P. Huhtanen. 2002. Evaluation of isoleucine, leucine, and valine as a second-limiting amino acid for milk production in dairy cows fed grass silage diet. J. Dairy Sci. 85:1533–1545. https://doi.org/10.3168/jds.S0022-0302(02)74223-9.

Lapierre, H., G. E. Lobley, L. Doepel, G. Raggio, H. Rulquin, and S. Lemosquet. 2012. Triennial Lactation Symposium: Mammary metabolism of amino acids in dairy cows. J. Anim. Sci. 90:1708–1721. https://doi.org/10.2527/jas.2011-4645.

Laspiur, J. P., J. L. Burton, P. S. Weber, J. Moore, R. N. Kirkwood, and N. L. Trottier. 2009. Dietary protein intake and stage of lactation differentially modulate amino acid transporter mRNA abundance in porcine mammary tissue. J. Nutr. 139:1677–1684. https://doi.org/10.3945/jn.108.103549.

López, A., N. Torres, V. Ortiz, G. Aleman, R. Hernandez-Pando, and A. R. Tovar. 2006. Characterization and regulation of the gene expression of amino acid transport system A (SNAT2) in rat mammary gland. Am. J. Physiol. Endocrinol. Metab. 291:E1059–E1066. https://doi.org/10.1152/ajpendo.00062.2006.

Mizushima, N. 2011. Autophagy in protein and organelle turnover. Cold Spring Harb. Symp. Quant. Biol. 76:397–402. https://doi.org/10.1101/sqb.2011.76.011023.

Nicklin, P., P. Bergman, B. Zhang, E. Triantafellow, H. Wang, B. Nyfeler, H. Yang, M. Hild, C. Kung, C. Wilson, V. E. Myer, J. P. MacKeigan, J. A. Porter, Y. K. Wang, L. C. Cantley, P. M. Finan, and L. O. Murphy. 2009. Bidirectional transport of amino acids regulates mTOR and autophagy. Cell 136:521–534. https://doi.org/10.1016/j.cell.2008.11.044.

NRC. 2001. Nutrient Requirements of Dairy Cattle. 7th rev. ed. Natl. Acad. Press.

Pocius, P. A., and C. R. Baumrucker. 1980. Amino acid uptake by bovine mammary slices. J. Dairy Sci. 63:746–749. https://doi.org/10.3168/jds.S0022-0302(80)83002-5.

Sharma, R., and V. K. Kansal. 2000. Heterogeneity of cationic amino acid transport systems in mouse mammary gland and their regulation by lactogenic hormones. J. Dairy Res. 67:21–30. https://doi.org/10.1017/S0022029999003994.

Shennan, D. B., and C. A. Boyd. 2014. The functional and molecular entities underlying amino acid and peptide transport by the mammary gland under different physiological and pathological conditions. J. Mammary Gland Biol. Neoplasia 19:19–33. https://doi.org/10.1007/s10911-013-9305-5.

Shennan, D. B., D. T. Calvert, M. T. Travers, Y. Kudo, and C. A. Boyd. 2002. A study of L-leucine, L-phenylalanine and L-alanine transport in the perfused rat mammary gland: Possible involvement of LAT1 and LAT2. Biochim. Biophys. Acta 1564:133–139. https://doi.org/10.1016/S0005-2736(02)00410-8.

Sinclair, K. D., P. C. Garnsworthy, G. E. Mann, and L. A. Sinclair. 2014. Reducing dietary protein in dairy cow diets: Implications for nitrogen utilization, milk production, welfare and fertility. Animal 8:262–274. https://doi.org/10.1017/S1751731113002139.

Smith, P. K., R. I. Krohn, G. T. Hermanson, A. K. Mallia, F. H. Gartner, M. D. Provenzano, E. K. Fujimoto, N. M. Goeke, B. J. Olson, and D. C. Klenk. 1985. Measurement of protein using bicinchoninic acid. Anal. Biochem. 150:76–85. https://doi.org/10.1016/0003-2697(85)90442-7.

Soetaert, K., and T. Petzoldt. 2010. Inverse modelling, sensitivity, and Monte Carlo analysis in R using package FME. In FME. Cran.R-project.

Swanepoel, N., P. H. Robinson, and L. J. Erasmus. 2016. Rumen microbial protein flow and plasma amino acid concentrations in early lactation multiparity Holstein cows fed commercial rations, and some relationships with dietary nutrients. Livest. Sci. 190:58–69. https://doi.org/10.1016/j.livsci.2016.06.001.

Taylor, P. M. 2014. Role of amino acid transporters in amino acid sensing. Am. J. Clin. Nutr. 99:223S–230S. https://doi.org/10.3945/ajcn.113.070086.

Tovar, A. R., E. Avila, S. DeSantiago, and N. Torres. 2000. Characterization of methylaminoisobutyric acid transport by system A in rat mammary gland. Metabolism 49:873–879. https://doi.org/10.1053/meta.2000.6731.

Van Amburgh, M. E., E. A. Collao-Saenz, R. J. Higgs, D. A. Ross, E. B. Recktenwald, E. Raffrenato, L. E. Chase, T. R. Overton, J. K. Mills, and A. Foskolos. 2015. The Cornell Net Carbohydrate and Protein System: Updates to the model and evaluation of version 6.5. J. Dairy Sci. 98:6361–6380. https://doi.org/10.3168/jds.2015-9378.

Whitelaw, F. G., J. S. Milne, E. R. Orskov, and J. S. Smith. 1986. The nitrogen and energy metabolism of lactating cows given abomasal infusions of casein. Br. J. Nutr. 55:537–556. https://doi.org/10.1079/BJN19860061.

Wu, G. 2013. Amino Acids. CRC Press.

Ye, J., W. Palm, M. Peng, B. King, T. Lindsten, M. O. Li, C. Koumenis, and C. B. Thompson. 2015. GCN2 sustains mTORC1 suppression upon amino acid deprivation by inducing Sestrin2. Genes Dev. 29:2331–2336. https://doi.org/10.1101/gad.269324.115.

Yoder, P. S., J. Castro, and M. D. Hanigan. 2016. Limitations of least cost diet optimization for profit maximization and environmental policy evaluations. Summaries of Communications of the 2016 Meeting of the Animal Science Modelling Group, Salt Lake City, UT. Can. J. Anim. Sci. 96:626–635.

Yoder, P. S., X. Huang, I. A. Teixeira, J. P. Cant, and M. D. Hanigan. 2020a. Effects of jugular infused methionine, lysine, and histidine as a group or leucine and isoleucine as a group on production and metabolism in lactating dairy cows. J. Dairy Sci. 103:2387–2404. https://doi.org/10.3168/jds.2019-17082.

Yoder, P. S., J. J. Castro, T. Ruiz-Cortes, and M. D. Hanigan. 2020b. An in vitro method for assessment of amino acid bidirectional transport and intracellular metabolic fluxes in mammary epithelial cells. J. Dairy Sci. 103:8948–8966. https://doi.org/10.3168/jds.2020-18155.

Zebisch, K., and M. Brandsch. 2013. Transport of L-proline by the proton-coupled amino acid transporter PAT2 in differentiated 3T3-L1 cells. Amino Acids 44:373–381. https://doi.org/10.1007/s00726-012-1340-9.